New Assignment of the Electronically Excited States of Anthracene-9,10-endoperoxide and Its Derivatives: A Critical Experimental and Theoretical Study†

Andreas Klein, Martin Kalb, and Murthy S. Gudipati*

Institut für Physikalische Chemie, Universität zu Köln, Luxemburger Straβe 116, D-50939 Köln, Germany

Received: December 18, 1998; In Final Form: March 11, 1999

Electronic absorption spectra between 20 000 and 62 000 cm^{-1} of anthracene-9,10-endoperoxide (APO), its 9,10-dimethyl derivative (DMAPO), and perdeutero-APO isolated in Ar matrices are presented. These spectra are interpreted with the help of semiempirical (INDO/S and CNDO/S) calculations of the electronically excited states. Both experimental and theoretical results lead to an unambiguous assignment of the electronic states of APO and its derivatives. Several higher excited singlet states with significant oscillator strengths have been observed for the first time. The present assignment disagrees with the so far accepted assignment of the electronic states of these APOs, namely, that the first excited singlet state (S_1) is located at 23 000 cm^{-1} and that the photocycloreversion occurs from the higher excited singlet state (S_2) at ∼36 000 cm^{-1}. In our new assignment, the first excited singlet state (S_1) is located at 36 360 cm^{-1} and the low-lying triplet states that are predicted by the semiempirical calculations and measured using the heavy atom effect of C_2H_5I solvent are located at ∼21 000 cm^{-1}. Thus, the present assignment shows that the photocycloreversion of these APOs is not an exception to Kasha's rule. The spectroscopic signature of APO and DMAPO is governed by the exciton-like interactions between the phenyl subunits, which is also reflected in the strikingly similar spectroscopic properties of an isoelectronic molecule of APO, namely, 9,10-dihydro-9,10-ethanoanthracene. Possible reasons for the misinterpretation and/or wrong generalizations carried out in earlier works have been discussed.

Introduction

Endoperoxides of aromatic molecules, especially of ortho fused benzinoids such as naphthalene, anthracene, tetracene, and their derivatives have been of significant interest for photochemists and spectroscopists over the past several decades. Three important aspects of this class of molecules make them special. These are (1) sensitized [4 + 2] cycloaddition of O_2 ($a^1\Delta_g$) to aromatic molecules to form the endoperoxides and the mechanistic aspects of this reaction,[1] (2) photocycloreversion of endoperoxides to aromatic molecules and O_2 ($a^1\Delta_g$) occurring adiabatically from the higher excited singlet states (S_n, $n \geq 2$),[2] and (3) generation of 1:1 contact complexes of O_2 and aromatic molecules in rigid matrices to study the molecular interactions in the excited states.[3] The second aspect received considerable attention of photochemists due to the fact that these endoperoxides seem to belong to the class of molecules whose behavior is a conspicuous exception to the well-known Kasha's rule,[4] which states: *the emitting electronic level of a given multiplicity is the lowest excited level of that multiplicity (regardless of which state of a given multiplicity is excited)*. Kasha's rule is founded on the fact that $S_n \rightarrow S_1$ and $T_n \rightarrow T_1$ internal conversion occurs at much faster time scale (<1 ps) compared to $S_1 \rightarrow S_0$ (∼ns) or $T_1 \rightarrow T_0$ (μs−s) deexcitation time scales. Though photochemical reactions are not explicitly considered by Kasha, photochemists invoke Kasha's rule to explain photochemical processes based on the same reasons. However, it should be kept in mind that if photochemical processes are fast enough to compete with internal conversion, photochemistry can occur from higher excited states and such cases are not in contradiction to the original Kasha's rule.

Historically, it was Kearns and Khan[5] who predicted in 1969 using state and orbital correlation diagrams that excitation of cyclopentadiene endoperoxide (CPO, 2,3-dioxabicyclo[2.2.1]-hept-5-ene) into S_1 or T_1 states leads to a barrierless O−O homolytic bond cleavage and that the cycloreversion from these states has to circumvent a barrier. However, a barrierless cycloreversion is predicted when CPO is excited into the higher singlet states (structures of the molecules discussed in this paper are given in Chart 1). These authors also generalized their predictions to aromatic endoperoxides and forecasted that the family of endoperoxides should undergo wavelength-dependent dual photochemistry. In agreement with their predictions, Rigaudy et al.[6] reported wavelength-dependent photochemistry of 9,10-diphenylanthracene-9,10-endoperoxide (DPAPO). They showed that irradiation at 253.7 nm leads to cycloreversion (major channel) and irradiation at longer wavelengths (>280 nm) to O−O homolysis products. With an elegantly designed experimental strategy Brauer and co-workers[7] have shown in 1980 that photocycloreversion of dibenzo[*aj*]perylene-8,16-dione endoperoxide (HCDPO) occurs from the S_2 state and not from the S_1 or the T_1 state. These three crucial findings, which were consistent with each other, have been generalized in the due course of time to the family of endoperoxides.[8]

In recent times, several picosecond time-resolved studies have been reported[2b,9] even using femtosecond pulses,[10] where unusually long raise times (40−95 ps) for the cycloreversion of aromatic endoperoxides have been observed, except in one case.[10] These observations have been interpreted as being due

* Corresponding author. Fax: +49-221-470-5144. E-mail: murthy@hartree.pc.uni-koeln.de.

† M.S.G. wishes to dedicate this publication to Professor Josef Michl on the occasion of his 60th Birthday.

10.1021/jp984792j CCC: $18.00
Published on Web 04/29/1999

CHART 1 Ab Initio (RHF/631G) Optimized Structures of Molecules Referred to in the Present Article[a]

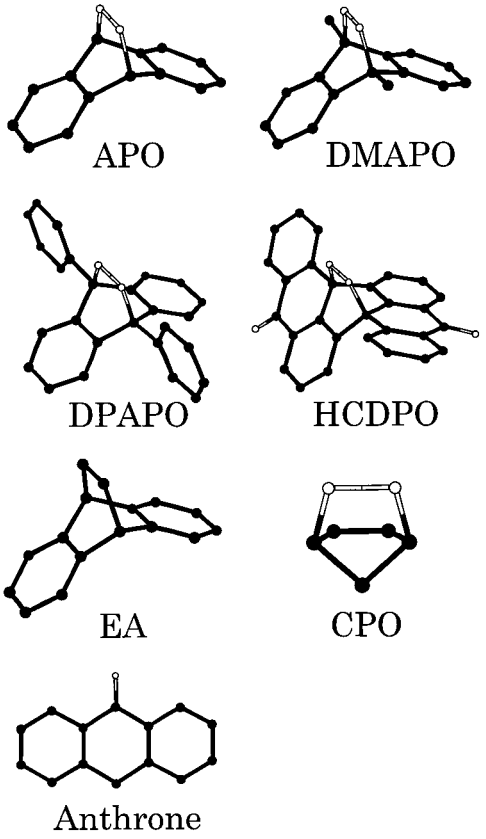

[a] Hydrogen atoms are not shown for clarity. Carbon atoms are represented by filled circles and oxygen atoms by open circles. APO = anthracene-9,10-endoperoxide; DMAPO = 9,10-dimethyl derivative of APO; DPAPO = 9,10-diphenyl derivative of APO; HCDPO = dibenzo[*aj*]perylene-8,16-dione endoperoxide; EA = 9,10-dihydro-9,10-ethanoanthracene; CPO = cyclopentadiene endoperoxide (2,3-dioxabicyclo[2.2.1]hepta-5-ene).

to the formation of a biradical intermediate through a nonconcerted cleavage of one of the C−O bonds[2b,9,10] and due to a barrier which slows down the cycloreversion during the second C−O bond cleavage. If it were to be a concerted and barrierless S_n ($n \geq 2$) photocycloreversion, then a much shorter raise time (<3 ps) is expected.[2b,9,10] Thus, presently it is believed that the photocycloreversion of endoperoxides occurs from higher excited singlet states (S_n, $n \geq 2$) in a nonconcerted fashion with a barrier at the last step of the reaction.

It is important to note here that since the work of Kearns and Khan no other theoretical investigation is reported to date, despite the intriguing exceptional behavior of the endoperoxides on one side and tremendous advances in theoretical methods on the other side. Further, so far there exists no experimental evidence for the dual photochemistry of CPO predicted by Kearns and Khan.

We have undertaken studies on anthracene-9,10-endoperoxide (APO), its 9,10-dimethyl derivative (DMAPO), and APO-d_{10} with the aim of generating 1:1 contact complexes in rare gas matrices and studying their interactions in the electronically excited states (aspect 3, vide supra), especially involving the higher excited states that are reached with vacuum-ultraviolet (VUV) photons. Thus, it was necessary to carry out systematic spectroscopic investigations on these endoperoxides in the VUV region (>100 nm) before we could proceed with the above-mentioned studies. Our theoretical and experimental investigations reported in this paper show that, at least in the case of APO and DMAPO, the well accepted S_2 photocycloreversion (aspect 2, vide supra) is wrong. This S_2 state is in fact the S_1 (first excited singlet) state with $S_1 \leftarrow S_0$ absorption at 275 nm, and hence the photocycloreversion of these endoperoxides is not an exception to Kasha's rule. For the first time, several higher excited singlet states of these peroxides between 220 and 160 nm with significant oscillator strengths will also be presented.

Experimental Section

APO, APO-d_{10}, and DMAPO were synthesized and purified using a method described in the literature.[11] The UV−vis absorption spectra (>200 nm) were recorded on a Perkin-Elmer-559 spectrometer. Poly(vinyl alcohol) (PVA) film was soaked in a 1 M solution of DMAPO in CH_2Cl_2 for 2 days and washed with CH_2Cl_2 several times before measuring the absorption spectrum. VUV spectra of the endoperoxides in Ar matrices deposited on a LiF window at 22 K were measured at the synchrotron radiation facility BESSY at Berlin, using the monochromators 1m-SEYA and 3m-NIM-1.[12] It is well-known that anthracene endoperoxides dissociate at elevated temperatures close to the melting point. For this reason, our initial attempts to obtain matrix-isolated APOs with the experimental setup used to generate matrix-isolated aromatic molecules[12] were unsuccessful, with which we needed to heat the sample around 150 °C (APO decomposes at 167 °C[13]). To avoid thermal decomposition of APOs, we have constructed an ultrahigh vacuum (UHV) sample feed through, which can be moved close to the matrix window (with a ∼6 cm distance between the sample holder and the matrix window) as shown in Figure 1. APOs were placed in a quartz crucible of 3 mm diameter and 5 mm height, which was inserted at the end of the sample feed through. The temperature at the sample can be controlled between −150 and 250 °C. Matrix gases (here Ar) were flown through a 3 mm metal tube and directed to pass over the top edge of the quartz crucible. The advantage of this setup is that the molecules that are heat-sublimed and carried with the Ar gas do not undergo collisions with any metal surface before getting deposited on to the matrix window. Additionally, due to direct sublimation of the sample close to the matrix window, sufficient quantities of the endoperoxides can be sublimed at much lower sample temperatures. The matrices were deposited at a sample temperature of 90−110 °C for 60 min (unless specified otherwise) at a background pressure of 1.5×10^{-5} mbar on the LiF window cooled to 22 K using a closed-cycle Helium cryostat (Air Products). After the deposition of the matrices the quartz crucible was cooled to −100 °C, the sample feed through was moved away from the matrix window and separated from the matrix chamber with a UHV valve. With this setup, we succeeded in obtaining optically transparent matrices without decomposing APOs. The vacuum in the sample chamber was less than 1×10^{-8} mbar during the measurements. Irradiation of the peroxides was carried out with a Nd:YAG (Continuum, Surelite-II-10, frequency tripled to 355 nm, 10 Hz, 5 ns pulses with a pulse energy of 150 mJ) pumped dye laser (Radiant Dyes, Narrow-Scan) at 275 nm after frequency doubling with a BBO crystal, with a pulse energy of ∼2 mJ. Transmission spectra were measured using a windowless GaAsP photodiode (Hamamatsu G1127-02, 100-680 nm), and the photodiode current was amplified using an electrometer (Keithley 616). Absorption spectra were calculated by ratioing the transmission spectra of the matrices with the spectrum of the LiF window measured before depositing the matrices. Fluorescence and excitation spectra were measured using a 0.5 m

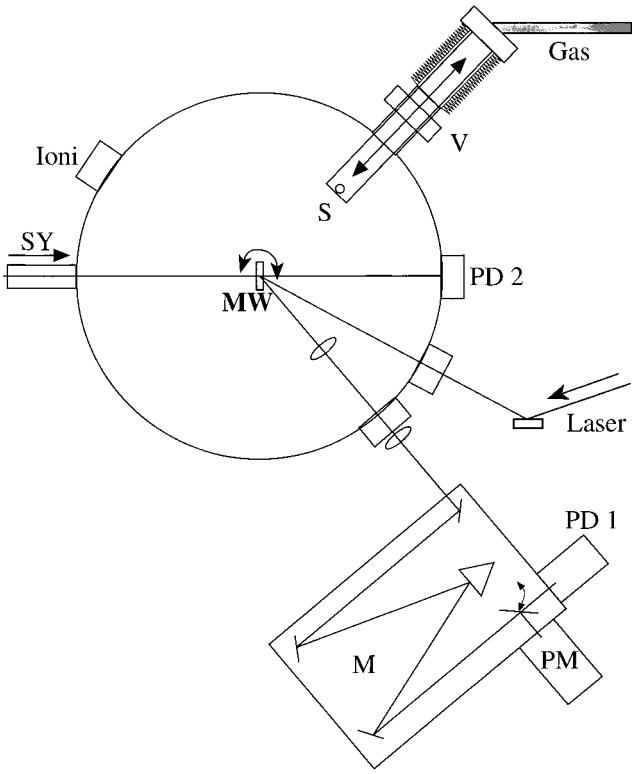

Figure 1. Schematic representation of the experimental setup. The large circle is the cylindrical matrix chamber under high vacuum: MW = matrix window (LiF); S = feed through for the sample that is placed at the tip of the feed through shown as a small open circle; V = UHV valve; Ioni = ionization gauge for determining the vacuum; SY = optical path of the synchrotron light under high vacuum. PD2 = GaAsP photodiode for absorption measurements; laser = optical path of the laser using a highly reflective UV mirror; M = 0.5 m emission monochromator equipped with GaAs photomultiplier (PM) and InGaAs photodiode (PD1). Emission is collimated and focused on to the entrance slits of M using planoconvex and double-convex quartz lenses. Straight lines indicate the optical paths.

monochromator (Acton Research) equipped with a GaAs photomultiplier (Hamamatsu, 180-950 nm) or an InGaAs photodiode (Opto-Electronics, 800−1600 nm) as shown in Figure 1.

Geometries of the molecules dealt in this paper were optimized with the ab initio program GAUSSIAN-94[14] using the restricted Hartree−Fock[15] (RHF) approximation and the 6-31G basis set. All parameters were optimized applying molecular symmetry restrictions. The optimized geometries were used to calculate the SCF-MOs and the spectroscopic properties of these molecules using the CNDO/S[16] and INDO/S[17] methods with singly (SCI) as well as singly and doubly excited (SDCI) configuration interactions (CI).[18] The two-center, two-electron integrals were evaluated using Pariser−Parr parameters. All the parameters used in CNDO/S and INDO/S methods are identical except for the empirical bonding parameter for carbon (β_C) which is −17.5 eV in CNDO/S and −16.0 eV in INDO/S computations. Further INDO/S includes the one-center exchange integrals G^1 and F^2.[17b] Since the one-center exchange integrals have only a minor effect on the singlet excitation energies, an INDO/S calculation including doubly excited configurations should predict singlet and triplet states with similar accuracy. The dimension of the CI matrix was typically 125 energy-selected configurations per irreducible representation of the corresponding molecular symmetry group, summing up, for example, to a total of 500 configurations in the case of molecules with C_{2v} symmetry.

TABLE 1: Geometric Parameters of APO and DMAPO Optimized with the ab Initio (RHF/6-31G) Method[a]

molecule	R_{O-O} [pm]	R_{C-O} [pm]	R_{C-R} [pm]	$\alpha_{O-C-C'}$ [deg]	$\theta_{C'-C-C''}$ [deg]	$\varphi_{C'-C-R}$ [deg]
APO	147 (148)	148 (148)	108	106.3	109.7	114.8
DMAPO	146	149	151	105.4	108.1	116.5

[a] Experimental values (ref 13) are given in parentheses. R = H or CH_3. C′ and C″ are the symmetry equivalent carbon atoms bonded to the bridge-head carbon, C.

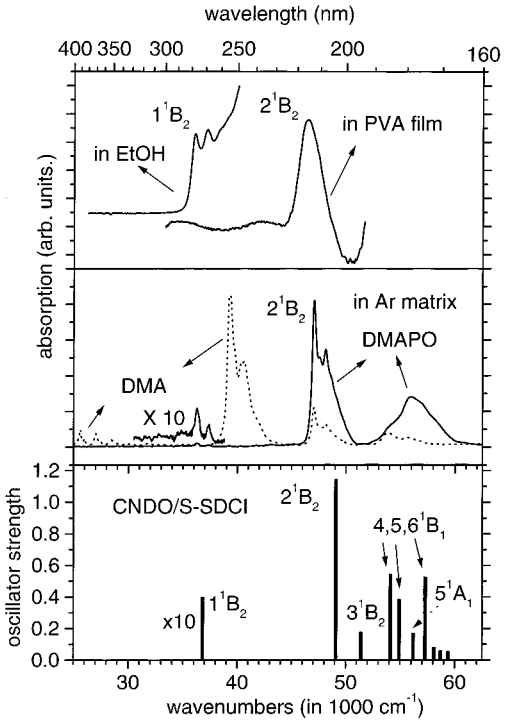

Figure 2. (top) Absorption spectra of DMAPO in ethanol and PVA film; (middle) absorption spectra of DMAPO isolated in Ar matrices before (—) and after (···) laser photolysis at 275 nm; (bottom) a bar graph of excitation energies and oscillator strengths of the singlet excited states of DMAPO using the CNDO/S−SDCI method.

Results

The optimized geometry of APO with the RHF/6-31G is in good agreement with the geometry derived from single-crystal X-ray diffraction analysis (Table 1).[13] To compare the reliability of the predicted excitation energies and oscillator strengths of transitions between the ground state and the exited states of endoperoxides, calculations were carried out using both CNDO/S and INDO/S methods with SCI and SDCI for all the molecules presented here. In Table 2, the computed spectroscopic data for DMAPO is presented. For singlet states, the predictions of all methods are generally good, whereas for triplet states, CNDO/S parameters tend to give higher energies by ca. 6000 cm^{-1}. The best matching between experimental and calculated energies is obtained using CNDO/S-SDCI for singlet states and INDO/S (SCI or SDCI) for triplet states. Absorption spectra of DMAPO in Ar matrix, in PVA-film, and a 10^{-3} M DMAPO in ethanol are shown in Figure 2 and compared with CNDO/S-SDCI predictions. Absorption spectra of APO and APO-d_{10} are shown in Figure 3 along with the semiempirical data. Absorption spectra of the endoperoxides in matrices shown in Figures 2 and 3 have been baseline corrected for the continuous increase in the scattering of the VUV light by the matrices toward shorter wavelengths. In Figure 4, changes in the absorption spectrum of DMAPO in an Ar matrx during laser

TABLE 2: Computed Excitation Energies (ΔE in 1000 cm^{-1}) of the Singlet and Triplet States and Oscillator Strengths of the Singlet States of DMAPO

INDO/S						CNDO/S					
SCI			SDCI			SCI			SDCI		
state	ΔE	f	state	ΔE	f	state	ΔE	f	state	ΔE	f
$^1B_2$	34.69	0.02	$^1B_2$	34.00	0.02	$^1B_2$	37.67	0.04	$^1B_2$	36.82	0.04
$^1A_1$	35.12	0.00	$^1A_1$	34.67	0.00	$^1A_1$	38.22	0.00	$^1A_1$	37.72	0.00
$^1A_2$	37.77	0.00	$^1A_2$	37.66	0.00	$^1A_2$	38.68	0.00	$^1A_2$	38.45	0.00
$^1B_1$	40.06	0.01	$^1B_1$	40.14	0.01	$^1B_1$	41.10	0.01	$^1B_1$	41.05	0.01
$^1B_2$	46.75	1.26	$^1A_2$	45.42	0.00	$^1B_2$	49.33	1.49	$^1A_2$	48.85	0.00
$^1A_2$	46.76	0.00	$^1B_1$	46.59	0.00	$^1A_2$	49.84	0.00	$^1B_2$	49.09	1.14
$^1B_2$	48.37	0.10	$^1B_2$	46.72	0.84	$^1B_2$	51.93	0.11	$^1B_1$	51.17	0.03
$^1A_2$	49.16	0.00	$^1A_2$	47.47	0.00	$^1A_2$	53.01	0.00	$^1B_2$	51.41	0.18
$^1B_1$	50.11	0.29	$^1B_2$	47.99	0.31	$^1B_1$	53.09	0.00	$^1A_2$	51.93	0.00
$^1A_2$	50.32	0.00	$^1A_2$	49.23	0.00	$^1A_1$	53.94	0.00	$^1B_1$	52.53	0.00
$^1B_1$	50.40	0.89	$^1B_1$	49.31	0.04	$^1B_1$	54.16	1.37	$^1A_2$	52.72	0.00
$^1A_1$	50.58	0.01	$^1A_2$	49.94	0.00	$^1B_1$	54.73	0.24	$^1A_1$	53.15	0.00
$^1A_1$	51.35	0.27	$^1A_1$	50.14	0.00	$^1A_2$	54.96	0.00	$^1B_1$	54.12	0.55
$^1B_1$	51.44	0.04	$^1B_1$	50.70	0.53	$^1A_1$	55.01	0.00	$^1A_1$	54.72	0.01
$^1B_1$	52.28	0.00	$^1B_1$	51.30	0.26	$^1B_2$	55.39	0.00	$^1B_1$	54.91	0.39
$^1B_2$	52.78	0.00	$^1A_1$	51.64	0.05	$^1A_1$	55.40	0.39	$^1A_2$	54.97	0.00
$^1A_2$	52.88	0.00	$^1A_1$	52.10	0.05	$^1B_1$	58.39	0.17	$^1B_2$	55.26	0.02
$^1A_1$	52.99	0.00	$^1B_1$	52.12	0.13	$^1A_2$	58.42	0.00	$^1A_1$	56.19	0.17
$^1A_1$	53.62	0.00	$^1B_2$	52.50	0.00	$^1A_1$	60.26	0.05	$^1B_2$	56.77	0.01
$^1B_2$	53.81	0.01	$^1A_2$	52.55	0.00	$^1B_1$	60.62	0.00	$^1B_1$	57.29	0.53
$^1A_2$	55.80	0.00	$^1B_2$	52.62	0.00	$^1A_2$	60.91	0.00	$^1A_1$	58.08	0.08
$^3A_2$	20.96		$^3A_2$	21.39		$^3A_2$	26.64		$^3A_2$	26.70	
$^3B_1$	21.34		$^3B_1$	21.73		$^3B_1$	27.22		$^3B_1$	27.40	
$^3B_2$	29.42		$^3B_2$	29.29		$^3B_2$	33.16		$^3B_2$	32.99	
$^3A_1$	29.69		$^3A_1$	29.59		$^3A_1$	33.58		$^3A_1$	33.41	
$^3A_2$	30.27		$^3A_2$	30.21		$^3A_2$	34.49		$^3A_2$	34.22	
$^3B_1$	30.51		$^3B_1$	30.47		$^3B_1$	34.76		$^3B_1$	34.63	
$^3B_2$	35.32		$^3B_2$	35.20		$^3B_2$	38.76		$^3B_2$	38.60	
$^3A_1$	35.55		$^3A_1$	35.45		$^3A_1$	38.99		$^3A_1$	38.81	

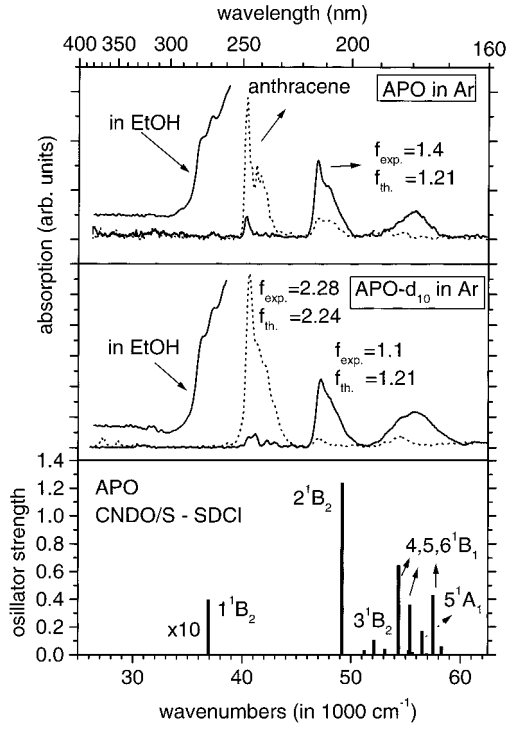

Figure 3. (top) Absorption spectra of APO isolated in Ar matrices before (—) and after (•••) laser photolysis at 275 nm; (middle) absorption spectra of APO-d_{10} isolated in Ar matrices before (—) and after (•••) laser photolysis at 275 nm; (bottom) a bar graph of excitation energies and oscillator strengths of the singlet excited states of APO using the CNDO/S-SDCI method. Absorption spectra measured in ethanol are also shown in the top and middle parts. Experimental oscillator strengths for the $2^1B_2 \leftarrow 1^1A_1$ transition at 47 000 cm^{-1} are also given (for details please refer the text).

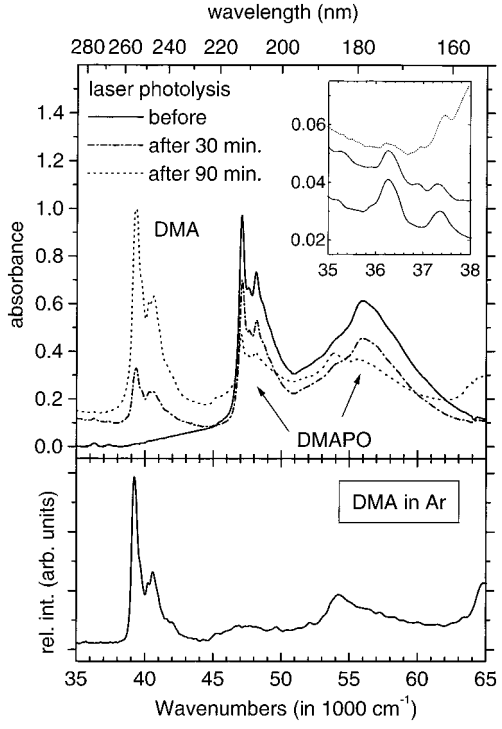

Figure 4. (top) Changes in the absorption spectra during the laser photolysis of DMAPO in an Ar matrix. The region between 35 000 and 38 000 cm^{-1} is shown enlarged as an insert. (bottom) Excitation spectrum of DMA (9,10-dimethylanthracene) isolated in Ar matrices by monitoring the fluorescence of DMA at 392 nm. An increase in the absorption bands of DMA and a decrease in the absorption bands of DMAPO with photolysis time can be clearly seen in the top part of the figure.

photolysis at 275 nm are shown, where a systematic decrease in the absorption bands of DMAPO and an increase in the absorption band of DMA are clearly observed. Excited singlet states, their energies, and oscillator strengths (f) of APO computed using the semiempirical methods described above are

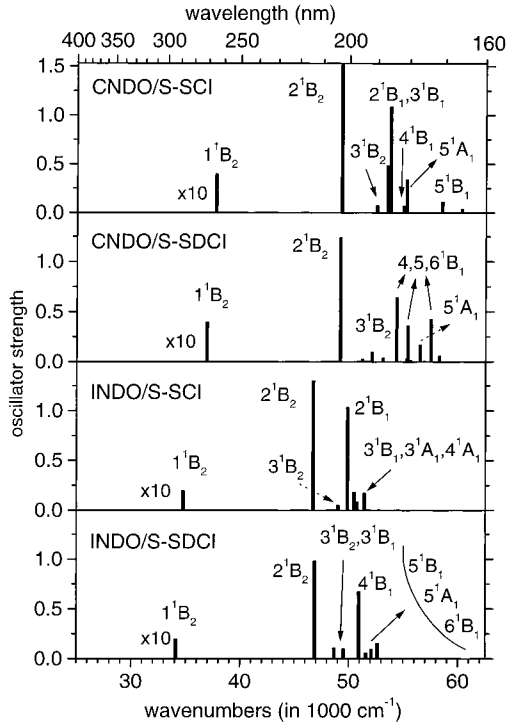

Figure 5. Bar graphs of the excitation energies and oscillator strengths of the singlet excited states of APO computed with different semiempirical methods are shown.

TABLE 3: Computed (CNDO/S−SDCI) Excitation Energies (ΔE in 1000 cm^{-1}) of the Singlet and Triplet States and Oscillator Strengths of the Singlet States of APO and EA Compared with the Literature Values of Benzene[26]

benzene			APO			EA		
state	ΔE	f	state	ΔE	f	state	ΔE	f
$^1B_{2u}$	39.52	0.00	$^1B_2$	36.92	0.04	$^1B_2$	36.09	0.05
			$^1A_1$	37.77	0.00	$^1A_1$	37.21	0.00
$^1B_{1u}$	50.00	0.00	$^1A_2$	38.65	0.00	$^1A_2$	38.16	0.00
			$^1B_1$	41.08	0.01	$^1B_1$	40.36	0.01
$^1E_{1u}$	55.97	1.25	$^1A_2$	49.08	0.00	$^1A_2$	48.45	0.00
$^1E_{2g}$	62.91	0.00	$^1B_2$	49.19	1.21	$^1B_2$	49.30	1.31
			$^1B_1$	51.24	0.03	$^1B_1$	50.45	0.02
			$^1A_2$	51.99	0.00	$^1A_2$	51.05	0.00
			$^1B_2$	52.12	0.10	$^1B_1$	52.29	0.05
			$^1B_1$	53.12	0.04	$^1A_2$	53.64	0.00
			$^1A_2$	53.37	0.00	$^1B_2$	53.92	0.03
			$^1A_1$	53.87	0.00	$^1A_1$	54.15	0.00
			$^1B_1$	54.36	0.65	$^1B_1$	54.17	1.26
			$^1A_1$	55.30	0.03	$^1B_2$	54.83	0.04
			$^1B_1$	55.39	0.36	$^1A_1$	55.01	0.07
			$^1A_2$	55.49	0.00	$^1A_2$	55.42	0.00
			$^1B_2$	55.61	0.02	$^1B_1$	55.67	0.05
			$^1A_1$	56.51	0.17	$^1B_1$	56.02	0.01
			$^1B_2$	56.90	0.01	$^1B_2$	56.15	0.02
			$^1B_1$	57.50	0.43	$^1A_1$	56.55	0.12
			$^1A_1$	58.27	0.06	$^1A_2$	56.92	0.00
						$^1A_1$	56.94	0.20
$^3B_{1u}$	31.78		$^3A_2$	26.64		$^3A_2$	26.43	
			$^3B_1$	27.31		$^3B_1$	26.79	
$^3E_{1u}$	38.39		$^3B_2$	33.06		$^3B_2$	32.40	
			$^3A_1$	33.43		$^3A_1$	32.65	
			$^3A_2$	34.28		$^3A_2$	33.94	
			$^3B_1$	34.64		$^3B_1$	34.77	
$^3B_{2u}$	35.38		$^3B_2$	38.65		$^3B_2$	38.83	
			$^3A_1$	38.84		$^3A_1$	39.04	

collected together as bar graphs in Figure 5. In Table 3, the electronic states of benzene are compared with those states of APO and its isoelectronic molecule 9,10-dihydro-9,10-ethanoanthracene (EA). Other results shown in the rest of the figures and tables are described at appropriate contexts in the discussion.

Discussion

1. Assignment of the Spectra. *Singlet States.* As we are dealing with a well accepted assignment which will be shown to be incorrect, it is necessary to take utmost precaution and check the internal consistency of the experimental and theoretical data. For this reason, we critically evaluate at each stage our results in the following.

The semiempirical results collected in Table 2 clearly show that the first excited singlet state (S_1) of DMAPO is of B_2 symmetry and is located around 36 000 cm^{-1}. This transition is associated with a weak oscillator strength of 0.02−0.04, in agreement with the weak molar extinction coefficient (ϵ) of ∼850 M^{-1} cm^{-1} of this transition.[19] If the existing assignment were to be correct, then the energy of the 1^1B_2 state is overestimated by theory to an extent of 13 000 cm^{-1} when compared to the assignment of the S_1 state of APO and DMAPO at ∼23 000 cm^{-1} by Brauer and co-workers.[19] We have computed excited singlet states of several planar aromatic molecules[20] and nonplanar multichromophoric systems containing aromatic subunits[21] using CNDO/S and INDO/S methods. These theoretical predictions on a number of molecules correlate with the experimental results up to an energy of 70 000 cm^{-1}, *without any exception*, within a maximum error of 0.6 eV (∼5000 cm^{-1}) in the transition energies. The semiempirical results are excellently comparable with the predictions of the best ab initio methods developed by Roos and co-workers,[22] which is clearly demonstrated even in the case of the weakly coupled aromatic molecule *E*-stilbene (Table 4). Thus, the predictions of semiempirical methods in the case of planar or nonplanar aromatic hydrocarbons are highly reliable. Similar conclusions have been derived by Thiel and co-workers[23] for several $\pi\pi^*$ and $n\pi^*$ vertical excitations in planar organic molecules using semiempirical methods. However, to the best of our knowledge, there are no examples known in the literature, where predictions of semiempirical methods have been systematically compared with experimental results for nonplanar and heterosubstituted systems such as APOs. If the predictions of the semiempirical methods parametrized for spectroscopic data (i.e., CNDO/S, INDO/S, etc.) in the case of APO and DMAPO were to be wrong, then this is the first time that these methods have miserably failed to predict the electronically excited states of medium-sized molecules containing aromatic units correctly. However, as will be shown below, this is not the case. What is important to note here is that calculations predict a strongly dipole-allowed transition ($2^1B_2 \leftarrow 1^1A_1$) at ca. 49 000 cm^{-1} with an oscillator strength of ∼1.2 in APO and DMAPO (Tables 2 and 3). Though Brauer and co-workers[19] have indicated the existence of S_3 at 40 000 cm^{-1}, so far the absorption spectra or an unambiguous assignment of the singlet states above 40 000 cm^{-1} are not known for these molecules. As can be seen in Figures 2 and 3, we observed this transition into the 2^1B_2 state at 47 000 cm^{-1} as the most significant feature of the absorption spectrum of APOs. The transition energy to this 2^1B_2 state is marginally overestimated by CNDO/S parametrization by about 2000 cm^{-1} and underestimated by only about 350 cm^{-1} by INDO/S parametrization. The same trend is also reflected in the energies of the 1^1B_2 state (Tables 2 and 3). Such a trend has also been observed by us for bichromophoric nonplanar molecules with C_{2v} molecular symmetry.[21]

Above 50 000 cm^{-1}, the semiempirical results tend to be less consistent, the major difference being the excitation energies predicted by CNDO/S and INDO/S methods. CNDO/S predicts several singlet states with significant oscillator strengths between 54 000 and 58 000 cm^{-1}, whereas when INDO/S is used these

TABLE 4: Comparison between the Semiempirical and ab Initio Predictions of the Excited Singlet States of *E*-Stilbene

state[a]	experiment[b] (in Ar matrix)		CNDO/S-SDCI[b]			CASPT2(MOLCAS)[c]		
(^1B_u)	ΔE/cm^{-1}	φ_{rel}[d]	ΔE/cm^{-1}	f	φ_{rel}[d]	ΔE/cm^{-1}	f	φ_{rel}[d]
A	31700		32200	1.01		32827	0.723	
B	43200	65 ± 10	45000	0.47	72	43715	0.371	46
C	51200	2 ± 8	48500	0.57	2	47990	0.524	9
D	59000	75 ± 10	56500	0.83	68	-	-	-

[a] All the states are of B_u symmetry (molecular symmetry C_{2h}); for the notation of the states, see refs 20c and 22. [b] Reference 20c. [c] Reference 22. [d] Relative direction of the transition moment of excitation with respect to the fluorescence transition moment.

states lie between 50 000 and 54 000 cm^{-1}. We have already mentioned earlier that INDO/S tends to predict lower excitation energies, and the difference of about 4000 cm^{-1} between CNDO/S and INDO/S is still acceptable. Moreover, all four different computations (Tables 2) are consistent among each other in predicting $^1B_1$ states being the dominant states in this region. In the absorption spectra of APO, APO-d_{10}, and DMAPO, a broad structureless band centered at 56 000 cm^{-1} with a shoulder at 53 800 cm^{-1} is observed (Figures 2 and 3). We assign this absorption as being mainly due to the $^1B_1 \leftarrow 1^1A_1$ transitions involving the higher excited $^1B_1$ states predicted by semiempirical calculations. For a better visualization, bar graphs of the excitation energies and oscillator strengths of the excited singlet states of APO computed using CNDO/S and INDO/S methods with SCI and SDCI are shown in Figure 5. A comparison between the spectra and the theoretical data shown in Figures 2, 3, and 5 clearly demonstrates that S_1 of APO (APO-d_{10}) and DMAPO is indeed located at 36 000 cm^{-1}, not at 23 000 cm^{-1} as has been assigned earlier.[19] The ratio of the integrated intensities of the band at 49 000 cm^{-1} and the two bands at 36 000 cm^{-1} is 175:1 compared to the ratios of the respective oscillator strengths 35:1 predicted by CNDO/S and 60:1 by INDO/S calculations. It should be kept in mind that the oscillator strengths predicted by the semiempirical methods of weakly allowed transitions tend to be less accurate than the strongly allowed transitions.

As we did not observe any luminescence from APOs when excited at 36 360 or 47 000 or 56 000 cm^{-1} in agreement with earlier observations,[7] we have carried out photolysis experiments to get further information on the nature of the absorption spectra shown in Figures 2 and 3 of APOs, whether they belong to the same species. In Figure 4, the absorption spectra of DMAPO in an Ar matrix that was prepared by heating the sample at 120 °C with a deposition time of 90 min is shown. We have used these experimental conditions in order to clearly measure the weak absorption around 36 000 cm^{-1} and measure its intensity changes during the laser photolysis and compare these changes with the changes in the absorption in the 47 000 cm^{-1} region. From the integrated intensities we find that the absorption band at 36 360 cm^{-1} is reduced by 48%, the absorption band at 47 000 cm^{-1} by 32%, and the absorption band at 56 000 cm^{-1} by 35% after 30 min of photolysis, compared to the integrated intensities of the respective bands before the photolysis. At the same time, the absorption of 9,10-dimethyl anthracene (DMA, one of the products of photocycloreversion) at 39 500 cm^{-1} is clearly seen in the spectrum measured after 30 min of photolysis. For comparison, an excitation spectrum of pure DMA deposited in an Ar matrix by monitoring the fluorescence of DMA at 392 nm is also shown in the bottom part of Figure 4. This spectrum is nearly identical to the excitation spectrum of anthracene, which we analyzed and reported earlier.[20a] The excitation energies of the corresponding transitions in DMA are shifted to lower energies compared to those of anthracene. The absorption spectra of DMA isolated in Ar and DMA generated through the photolysis of DMAPO in Ar (Figure 4) compare excellently with each other including a clearly visible shoulder at 54 000 cm^{-1} after 90 min of photolysis of DMAPO (Figure 4, dotted spectrum). We notice further decrease in the absorption bands at 36 360, 47 000, and 56 000 cm^{-1} and further increase in the absorption of DMA at 39 500 cm^{-1} after 90 min photolysis. Thus, in due course of photolysis, the absorption spectra between 45 000 and 60 000 cm^{-1} not only contain the absorption bands of DMAPO but also bands due to DMA generated during the photolysis. Keeping in mind the weak nature of the absorption at 36 360 cm^{-1} and the absorption bands of DMA between 45 000 and 60 000 cm^{-1}, the integrated absorption intensities given above clearly demonstrate that all the three absorption bands at 36 360, 47 000, and 56 000 cm^{-1} indeed belong to DMAPO and the product of cycloreversion is predominantly DMA. Absorption of O_2, which is generated along with DMA is difficult to quantify due to its broad and structureless absorption[12] with a maximum at 66 000 cm^{-1}. Evidence for O_2 being the second photoproduct is derived from the fact that, after the photolysis of DMAPO, the DMA molecules generated did not fluoresce when excited at 39 500 cm^{-1} into the B_b absorption band. This is due to efficient quenching of the excited DMA by O_2, both of which are the products of photocycloreversion existing in the mother cage of the Ar matrix. These observations are in agreement with earlier studies on APOs in organic glasses at 77 K.[3] Warming the matrices to 30 K resulted in a substantial increase in the fluorescence of DMA, whereas the absorption of DMA remained unchanged indicating the mobility of O_2 away from DMA. Similar behavior is also observed with APO and APO-d_{10}.

The experimental and theoretical data presented and discussed so far are consistent with each other and show that the S_1 state of APO, APO-d_{10}, and DMAPO is located around 36 000 cm^{-1}. We have shown further that photolysis of these endoperoxides at 275 nm results in cycloreversion to the corresponding anthracene and O_2, in agreement with earlier observations.[19] Under matrix-isolated conditions, the absolute concentration of the solute molecules in the matrix is not known and consequently the oscillator strength of a particular transition cannot be determined by simply integrating the absorption band. However, by assuming that photolysis at 275 nm of each endoperoxide molecule produces one anthracene molecule and one O_2 molecule, it is possible to derive the experimental oscillator strength of the $2^1B_2 \leftarrow 1^1A_1$ transition of the endoperoxides at 47 000 cm^{-1} by using the known experimental and theoretical oscillator strength of the B_b transition (39 500 cm^{-1}) of anthracene.[20a] We have integrated the regions of the spectra of APO and APO-d_{10} shown in Figure 3 from 38 000 to 44 000 cm^{-1} and from 45 000 to 51 000 cm^{-1} before and after the nearly complete photolysis of APO and APO-d_{10}. From these intensities we could roughly estimate the oscillator strength of the $2^1B_2 \leftarrow 1^1A_1$ transition of APO to be 1.4 and APO-d_{10} to be 1.1. These values are in excellent agreement with the values predicted by the semiempirical methods for this transition around 1.2 (Tables 2 and 3, Figure 3).

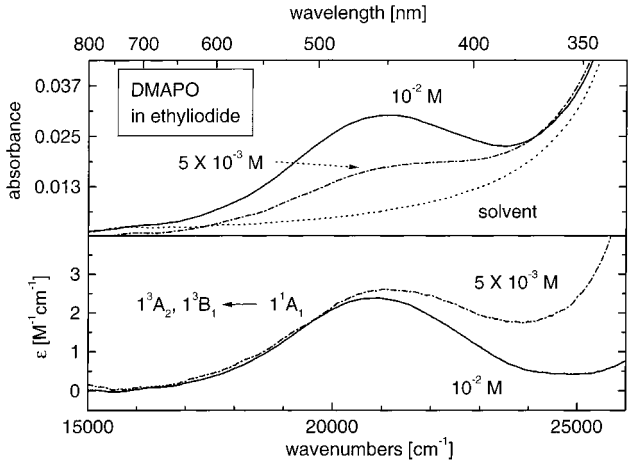

Figure 6. Heavy atom induced singlet−triplet absorption spectra of DMAPO in ethyl iodide at 5×10^{-3} M and 10^{-2} M concentrations (top). For comparison, the absorption spectrum of the solvent is also shown. In the bottom these spectra, after subtracting the solvent spectrum in ϵ units, are shown.

In conclusion, the repeated consistency between theoretical predictions and experimental observations presented here leads to an unambiguous assignment of the electronically excited singlet states of APO, APO-d_{10}, and DMAPO, and hence we assign the S_1 state of these endoperoxides to the transition at 36 000 cm^{-1}.

Triplet States. Dual photochemistry of APOs mentioned in the Introduction establishes that the cycloreversion of APOs occurs only when excited at shorter wavelengths than 280 nm[6,19] and we have shown in the previous section that it is the S_1 state which is reached at this wavelength. Then the question remains, why does at longer wavelengths the homolytic O−O bond cleavage occur. In the literature, though S_1 state photochemistry has wrongly been attributed for this reaction pathway,[19] so far no evidence against the involvement of the triplet states has been reported. We have used the well-known external heavy atom effect to enhance the singlet−triplet transition probability, and the results are discussed below. Absorption spectra were measured in iodoethane (C_2H_5I) as well as in bromoethane (C_2H_5Br) from APO and DMAPO at different concentrations. During the measurements, we realized that APO is destroyed in the solution at a faster rate, which led to inconsistent absorption spectra over several attempts. With 5×10^{-3} M or 10^{-2} M DMAPO in C_2H_5Br we could not observe significant heavy atom effect above the detection limit of the spectrometer. However, we could measure good quality spectra of 5×10^{-3} M and 10^{-2} M DMAPO in C_2H_5I. These spectra are shown in Figure 6. We clearly find a broad absorption centered around 21 000 cm^{-1} with an ϵ value of $\sim$3 M^{-1} cm^{-1}. Such small ϵ values are typical for forbidden singlet−triplet transitions induced by heavy atom effect.[24] The semiempirical calculations predict two closely spaced triplet states, $^3A_2$ as the first and $^3B_1$ as the second, around 21 000 cm^{-1} (INDO/S). The energies of the triplet states are unusually and systematically overestimated by the CNDO/S method by $\sim$6000 cm^{-1} for all the systems investigated in the present study. On the basis of these observations and on our assignment of the S_1 state of these endoperoxides at 36 000 cm^{-1}, we propose that the homolytic O−O bond cleavage of these endoperoxides should occur in the triplet manifold.

2. Exciton Interactions. A closer look at the symmetries of the low-lying excited singlet and triplet states of APO and DMAPO reveals that these states are indeed correlated to the corresponding states of the benzene subunit. Exciton, exchange (due to through-space overlap of the MOs of monomer units), and through-bond interactions in bichromophoric systems are well-known,[25] and we have recently analyzed these interactions using semiempirical methods.[21] Each electronic excited state of the monomeric unit splits into n states in a *supermolecule* containing n monomeric units. The magnitude of the splitting energy is governed by the energy and oscillator strength (f) of the transition in the monomer, the mutual orientation of the monomers, and the distance between the centers of the monomers.[21,25] In the present context, the first two excited singlet states of the monomer (benzene) are the $^1B_{2u}$ and $^1B_{1u}$, respectively.[26] The B_{2u} state of benzene (D_{6h} symmetry) splits into B_2 and A_1 states in APOs (C_{2v} symmetry). Similarly, the B_{1u} state of benzene splits into A_2 and B_1 states in APOs. Thus, the first four excited singlet states of APO and DMAPO are indeed $^1B_2$, $^1A_1$, $^1A_2$, and $^1B_1$, respectively, as can be seen in Tables 2 and 3. The transitions into the first two excited singlet states in benzene are symmetry forbidden, and for this reason, the corresponding states (except A_2, which is symmetry forbidden) in APO, though symmetry allowed, are still weak transitions. The doubly degenerate states of benzene of E symmetry split into B_2, A_1, A_2, and B_1 states in APO. Thus, the next two singlet excited states of benzene ($^1E_{2g}$ and $^1E_{1u}$) split into four singlet states each. The symmetry allowed E_{1u} state of benzene results in stabilized $^1B_2$ around 47 000 cm^{-1} and destabilized $^1A_1$ and $^1B_1$ states around 56 000 cm^{-1} in APO (Tables 2 and 3). It should be noted that a direct correlation of the higher excited singlet states of benzene and APO is not straightforward because of further interactions between the closely lying states of the same symmetry with each other. Another important aspect to be mentioned here is that in molecules such as APOs, with direct orbital overlap between monomeric units, exchange interactions become significant and the electronic states of the *supermolecule* are no longer completely described by the exciton interactions alone.[21] Thus, the assignment of the origins of the higher excited states is only qualitative. These exciton-like interactions can also be clearly observed in the triplet states. The first three triplet states of benzene are $^3B_{1u}$, $^3E_{1u}$, and $^3B_{2u}$, respectively.[23,26] These states correlate to $^3A_2$, $^3B_1$; $^3B_2$, $^3A_1$, $^3A_2$, $^3B_1$; and $^3B_2$, $^3A_1$, respectively, of APOs, as can be seen in Tables 2 and 3.

The analysis presented above clearly shows that for the low-lying singlet and triplet excited states, oxygen atoms in APO and DMAPO are only spectators and the spectroscopic signature is governed by the exciton-like interactions between the aromatic rings. Transitions into the higher excited states may have contributions from oxygen atoms. Hence, the photochemistry of APO and DMAPO should occur only as a secondary aspect, as a consequence of the evolution of the corresponding excited states in which the excitation is initially localized on the phenyl rings.

Inspired by the above unanticipated and compelling findings, we have computed the electronic states of 9,10-dihydro-9,10-ethanoanthracene (EA), an isoelectronic molecule of APO, which is similar to APO with respect to the geometrical disposition of the aromatic rings and in which the O−O (endoperoxide) bridge of APO is replaced by the H_2C-CH_2 (ethano) bridge (Chart 1). The results are collected in Table 3 and compared with the electronic states of APO in Figure 7. An excellent agreement between the spectroscopic properties of APO and EA can be directly seen from Figure 7 and Table 3, including the symmetries, energies of the singlet and triplet states, and the oscillator strengths of the singlet states. The

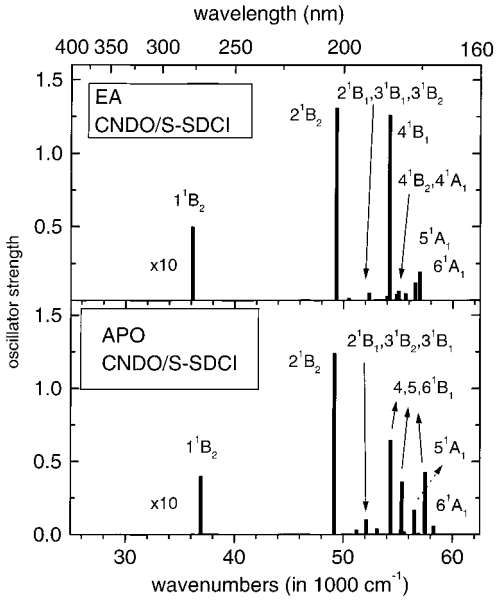

Figure 7. Comparison between the computed electronically excited singlet states of APO and EA (refer to Chart 1 for molecular structures).

experimental absorption maxima of 1,5-dideuterio-EA in isooctane are reported[27] at 36 765 cm^{-1} with $\epsilon = 1650$ M^{-1} cm^{-1} (APO at 36 360 cm^{-1}, $\epsilon = 850$ M^{-1} cm^{-1})[19] and at 49 020 cm^{-1} with $\epsilon = 35\,320$ M^{-1} cm^{-1} (APO at 47 000 cm^{-1}). For the second transition, the computed *f* values are very similar (Table 3). Fluorescence maximum of EA has been reported[28] to be at 34 965 cm^{-1} confirming that the absorption at 36 765 cm^{-1} of EA[28] and EA-d_2[27] is due to the $S_1 \leftarrow S_0$ transition. In conclusion, the spectroscopic properties of APO and DMAPO as well as EA are controlled by the exciton-like interactions between the aromatic rings and excitations into the low-lying singlet and triplet states occur within the aromatic rings.

3. Nature of the Excited States and Retrospection. *Analysis of the SCF-MOs.* In the literature[7-9] it is so far believed that excitation into the S_1 state at 23 000 cm^{-1} of APO has predominantly $\sigma^*_{OO} \leftarrow \pi^*_{OO}$ character, inferring that this excitation is mostly localized on the oxygen atoms. Excitation into the S_2 state, on the other hand, has been attributed with the $\pi^*_{CC} \leftarrow \pi_{CC}$ character, implying that this transition is mainly localized in the aromatic rings. We have analyzed the SCF-MOs computed using both ab initio and semiempirical (CNDO) methods of APO and DMAPO that are involved in the configurations that define the first excited singlet state (S_1) and some selected singlet and triplet states. The results for APO are given in Table 5, and the MOs are sketched in Figure 8. It is evident from Figure 8 that the MOs computed using ab initio and semiempirical methods are consistent with each other. The minor differences are the absolute energies of the MOs and an interchange of HOMO-2 and HOMO-3 between the ab initio and CNDO computations. As can be seen from Figure 8, the first four HOMOs and four LUMOs of APO do not contain any significant contribution from oxygen atoms. These eight MOs are predominantly involved in the transitions from the ground state to the low-lying singlet and triplet states, as given in Table 5. The highest HOMO with significant π^*_{OO} character is the HOMO-4 and this HOMO does not contribute to the lowest singlet or triplet states. Thus, none of the transitions into the low-lying singlet and triplet states has a significant $\sigma^*_{OO} \leftarrow \pi^*_{OO}$ character, and consequently, the S_1 state of APO and DMAPO assigned so far is neither an excited singlet state nor has a dominant $\sigma^*_{OO} \leftarrow \pi^*_{OO}$ character.

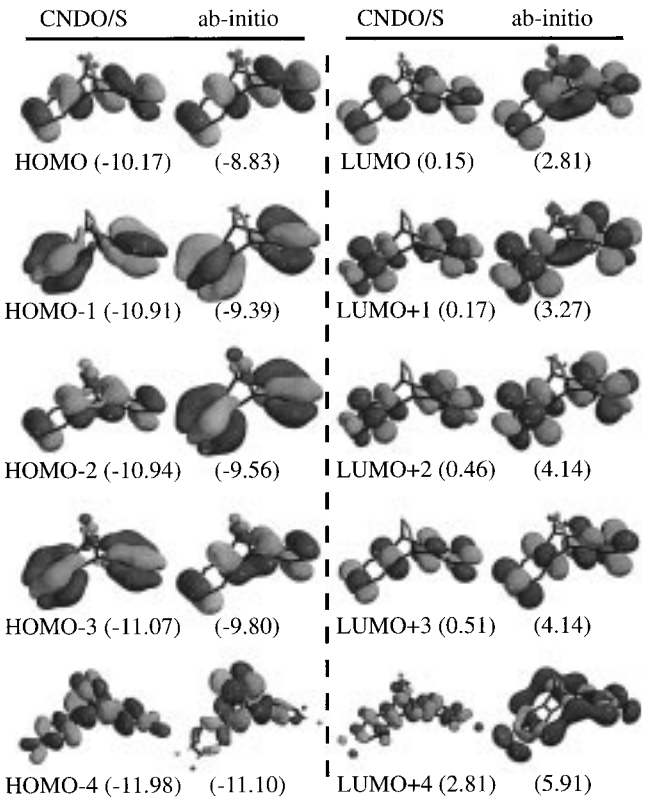

Figure 8. Selected set of SCF-MOs of APO computed using CNDO/S and ab initio methods. Energies of the MOs in electronvolts are given in parentheses. Orientation of the molecule is the same as shown in Chart 1. For clarity, H atoms were removed from the molecular skeleton but not the MO coefficients of H atoms, which are seen only in HOMO-4 and LUMO+4.

TABLE 5: Leading Configurations and the Coefficients (CNDO−SDCI) of the SCF-MOs for Some Selected Singlet and Triplet Excited States of APO

transition	ΔE	f	MO coefficients of leading configurations	
$1^1B_2 \leftarrow 1^1A_1$	36.92	0.04	HOMO → LUMO+1	48%
			HOMO-1 → LUMO	19%
			HOMO-2 → LUMO+2	18%
			HOMO-3 → LUMO+3	14%
$2^1A_1 \leftarrow 1^1A_1$	37.77	0.00	HOMO → LUMO+2	36%
			HOMO-3 → LUMO	22%
			HOMO-2 → LUMO+1	21%
			HOMO-1 → LUMO+3	18%
$2^1B_2 \leftarrow 1^1A_1$	49.19	1.21	HOMO-1 → LUMO	48%
			HOMO → LUMO+1	27%
			HOMO-3 → LUMO+3	14%
$1^3A_2 \leftarrow 1^1A_1$	26.64		HOMO → LUMO	46%
			HOMO-2 → LUMO+3	24%
			HOMO-1 → LUMO+1	14%
			HOMO-2 → LUMO+2	12%
$1^3B_1 \leftarrow 1^1A_1$	27.31		HOMO → LUMO+3	37%
			HOMO-2 → LUMO	29%
			HOMO-3 → LUMO+1	14%
			HOMO-1 → LUMO+2	14%

Retrospection. In this section, we shall consider where and why the misinterpretation occurred in the past literature. As mentioned in the Introduction, three crucial publications[5-7] contributed to the generalization that the photocycloreversion of aromatic endoperoxides occurs from the higher excited (S_n, $n \geq 2$) states.

First, we consider the work of Kearns and Khan,[5] who predicted using state and orbital correlation diagrams that the HOMO and LUMO of cyclopentadiene endoperoxide (CPO)

TABLE 6: Computed Excitation Energies (ΔE in 1000 cm^{-1}) of the Singlet and Triplet States and Oscillator Strengths of the Singlet States of CPO

INDO/S						CNDO/S					
SCI			SDCI			SCI			SDCI		
state	ΔE	f	state	ΔE	f	state	ΔE	f	state	ΔE	f
$^1A''$	46.65	0.27	$^1A''$	46.88	0.17	$^1A''$	45.88	0.29	$^1A''$	46.91	0.21
$^1A'$	53.67	0.01	$^1A''$	51.44	0.00	$^1A'$	56.79	0.01	$^1A'$	55.97	0.01
$^1A''$	54.17	0.00	$^1A'$	52.38	0.01	$^1A''$	61.86	0.00	$^1A''$	60.53	0.00
$^1A'$	59.83	0.02	$^1A'$	56.73	0.04	$^1A''$	64.22	0.00	$^1A''$	64.15	0.00
$^1A''$	62.25	0.01	$^1A''$	61.78	0.01	$^1A'$	71.11	0.08	$^1A'$	68.62	0.08
$^1A''$	68.83	0.00	$^1A'$	67.41	0.04	$^1A''$	73.26	0.01	$^1A''$	71.97	0.01
$^1A'$	69.89	0.01	$^1A''$	67.98	0.00	$^1A'$	75.66	0.01	$^1A'$	75.18	0.01
$^3A''$	20.40		$^3A''$	20.40		$^3A''$	26.55		$^3A''$	26.54	
$^3A''$	44.70		$^3A''$	44.30		$^3A'$	56.61		$^3A'$	55.97	
$^3A'$	51.97		$^3A'$	51.07		$^3A''$	61.83		$^3A''$	60.53	
$^3A'$	56.08		$^3A'$	54.57		$^3A''$	64.11		$^3A''$	64.04	
$^3A''$	59.56		$^3A''$	59.21		$^3A'$	70.92		$^3A'$	68.54	

TABLE 7: Leading Configurations and the Coefficients (CNDO−SDCI) of the SCF-MOs for Some Selected Singlet and Triplet Excited States of CPO

transition	DE	f	MO coefficients of the leading configurations	
$1^1A'' \leftarrow 1^1A'$	46.91	0.21	HOMO → LUMO	95%
$2^1A' \leftarrow 1^1A'$	55.97	0.01	HOMO-1 → LUMO	87%
			HOMO −5→ LUMO	7%
$2^1A'' \leftarrow 1^1A'$	60.53	0.00	HOMO → LUMO+1	87%
			HOMO → LUMO+4	8%
$3^1A'' \leftarrow 1^1A'$	64.15	0.00	HOMO-4→ LUMO	61%
			HOMO-2 → LUMO	29%
$3^1A' \leftarrow 1^1A'$	68.62	0.08	HOMO → LUMO+2	43%
			HOMO → LUMO+3	29%
			HOMO → LUMO+5	21%
$4^1A'' \leftarrow 1^1A'$	71.97	0.01	HOMO-2 → LUMO	62%
			HOMO-4→ LUMO	23%
			HOMO-6→ LUMO	8%
$1^3A'' \leftarrow 1^1A'$	26.54		HOMO → LUMO	99%
$1^3A' \leftarrow 1^1A'$	55.97		HOMO-1 → LUMO	87%
			HOMO-5→ LUMO	7%
$2^3A'' \leftarrow 1^1A'$	60.53		HOMO → LUMO+1	87%
			HOMO → LUMO+4	8%
$3^3A'' \leftarrow 1^1A'$	64.04		HOMO-4 → LUMO	59%
			HOMO-2 → LUMO	31%

have π^*_{OO} and σ^*_{OO} character, respectively, and the $S_1 \leftarrow S_0$ transition should have the $\sigma^*_{OO} \leftarrow \pi^*_{OO}$ character. We have analyzed the SCF-MOs of CPO and their contribution to the excited singlet states of this molecule. These results are summarized in Tables 6 and 7 and Figure 9. To our surprise, both the HOMO and LUMO of CPO are predominantly localized on the olefinic carbons and are of π and π^* character, respectively. A significant contribution of π^*_{OO} can be seen in HOMO-1 (second HOMO). The σ^*_{OO} type MO can be noticed in LUMO + 1 computed by the ab initio method. However, this MO does not contribute to the CI wave function of the lowest singlet and triplet excited states of CPO, which are dominated by the HOMO → LUMO excitation (Table 7). Similar to APO MOs, in CPO we notice an interchange of HOMO-2 and HOMO-3 between the ab initio and semiempirical computations. Thus, we are left with no other choice but to state that the assumption made by Kearns and Khan[5] that the HOMO and LUMO of CPO have π^*_{OO} and σ^*_{OO} character, respectively, is not correct.

The second point to be considered is the dual photochemistry of DPAPO (Chart 1) reported by Rigaudy et al.,[6] who observed photocycloreverison when irradiated at 280 nm or shorter wavelengths and O−O bond cleavage when irradiated at wavelengths longer than 280 nm. Our theoretical computations show that the electronic excited states of DPAPO compare

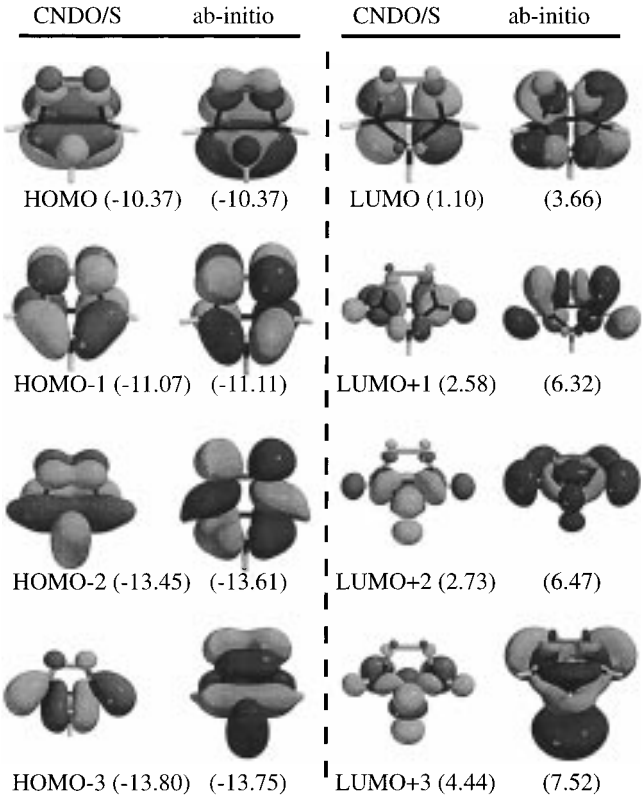

Figure 9. Selected set of SCF-MOs of CPO computed using CNDO/S and ab initio methods. Energies of the MOs in electronvolts are given in parentheses. Orientation of the molecule is the same as shown in Chart 1.

closely to the excited states of APO and DMAPO with respect to the excitation energies and oscillator strengths.[29] Thus, the photocycloreversion of DPAPO to DPA and O_2 should occur after exciting DPAPO into the S_1 state at shorter wavelengths than 280 nm. So far, there has been no experimental evidence against O−O bond cleavage to occur in the triplet manifold and hence this possibility cannot be ruled out in the case of long-wavelength photolysis of DPAPO. We propose that the dual photochemistry of DPAPO observed by Rigaudy et al. is photochemistry occurring in singlet and triplet manifolds, respectively.

We analyze now the spectra and the assignment of HCDPO (Chart 1) reported by Brauer and co-workers,[7] based on which the generalization on the S_n ($n \geq 2$) photocycloreversion of aromatic endoperoxides had been adopted in the literature. Brauer and co-workers clearly argued in their article that

TABLE 8: Computed Excitation Energies (ΔE in 1000 cm^{-1}) of the Singlet and Triplet States and Oscillator Strengths of the Singlet States of Anthrone and HCDPO Using CNDO/S−SDCI Method

anthrone			HCDPO		
state	ΔE	f	state	ΔE	f
$^1A_2$	26.60	0.00	^1B	30.12	0.00
			^1A	30.62	0.00
$^1A_1$	36.34	0.02	^1B	36.64	0.08
			^1A	37.47	0.01
$^1B_2$	36.95	0.00	^1B	38.15	0.05
			^1A	38.18	0.00
$^1B_2$	38.46	0.02	^1A	39.19	0.00
			^1B	40.36	0.02
$^1A_1$	40.29	0.01	^1A	40.96	0.01
			^1B	42.10	0.02
$^1B_1$	44.35	0.00	^1A	46.86	0.14
			^1B	48.51	1.18
$^1B_2$	46.88	1.25	^1B	50.18	2.98
			^1A	50.42	0.02
$^3A_1$	26.88		^3A	29.55	
			^3B	30.37	
$^3A_2$	26.89		^3B	30.68	
			^3A	30.69	
$^3B_2$	27.96		^3B	30.70	
			^3A	31.00	
$^3A_1$	31.65		^3B	31.65	
			^3A	32.17	

HCDPO can be looked at as two fused anthrone subunits containing the peroxide bridge, as can be seen from its structure (Chart 1). We have computed the singlet and triplet excited states of anthrone and HCDPO using both the CNDO/S and INDO/S methods. The results of CNDO/S-SDCI computations are shown in Table 8. In anthrone, the S_1 state (1^1A_2) is located at 26 600 cm^{-1} (C_{2v} molecular symmetry, x = out of plane axis; y = long in-plane axis; z = short in-plane axis). This state is associated with $p_x(\pi^*) \leftarrow p_y$ character of the carbonyl group, where an electron from the nonbonded p_y orbital of O is transferred into the π^* orbitals of the C atoms of the ring, a $\pi^* \leftarrow n$ transition involving the carbonyl group. The S_2 state (2^1A_1) has $\pi^* \leftarrow \pi$ character and is located at 36 340 cm^{-1}. The $S_1 \leftarrow S_0$ transition is symmetry forbidden, and the $S_2 \leftarrow S_0$ transition is associated with a weak oscillator strength. These properties of anthrone are in agreement with the literature reports.[7,30] HCDPO (C_2 symmetry) indeed behaves like a dianthrone, at least regarding its low-lying singlet and triplet states. The first two excited singlet states of HCDPO show predominant $\pi^* \leftarrow n$ character, similar to anthrone. If we invoke exciton-like analysis discussed in the previous section, then each excited state of anthrone (C_{2v} symmetry) splits into A and B states in HCDPO (C_2 symmetry). Thus, the 1^1A_2 state (S_1) of anthrone splits into 1^1B and 2^1A states in HCDPO. Computed energies of the first two (almost degenerate, Table 8) excited singlet states of HCDPO are around 30 000 cm^{-1} with $f = 0$. The S_2 state of anthrone (2^1A_1) splits into 2^1B and 3^1A states at 37 000 cm^{-1} in HCDPO, of which the 2^1B state is associated with an f value of 0.08. The absorption spectrum of HCDPO reported by Brauer and co-workers contains a vibronic progression starting at 25 800 cm^{-1} (ϵ = 52 M^{-1} cm^{-1}) which has been assigned by these authors to the $S_1 \leftarrow S_0$ transition. A second band at 30 700 cm^{-1} (ϵ = 3550 M^{-1} cm^{-1}) is assigned to the $S_2 \leftarrow S_0$ transition by the same authors. Our computed energies for these two absorption bands are overestimated by ~5000 cm^{-1}, as can be seen from Table 8. Keeping aside the exact assignment of the transition at 30 700 cm^{-1} to the S_3 (2^1B) state, semiempirical predictions agree with the assignment of Brauer and co-workers that the S_1 state of HCDPO is located around 26 000 cm^{-1} and the higher excited singlet states are responsible for the band at 30 700 cm^{-1}. Thus, the photocycloreversion and consequently the significant quantum yields of the production of $^1O_2$ observed when HCDPO was irradiated at higher energies than 30 000 cm^{-1} by Brauer and co-workers[7] may be an example of photochemistry from higher excited states. However, it should be kept in mind that excitation into the first two excited singlet states of HCDPO has the $\pi^* \leftarrow n$ character involving the carbonyl groups of the anthrone subunits. The absence of a carbonyl group in APO, DMAPO, and even DPAPO deprives these molecules of the low-lying excited states with $\pi^* \leftarrow n$ character involving the carbonyl group. Hence, though the observations and assignment of Brauer and co-workers regarding the photochemistry of HCDPO may be correct, generalization of the spectroscopic and photochemical properties of HCDPO to other aromatic endoperoxides that contain no carbonyl group, like APO, DMAPO, and DPAPO, is wrong.

Conclusions

In this article we have presented absorption spectra of APO, APO-d_{10}, and DMAPO that span into the VUV region up to 160 nm. The assignment of these spectra has been given by comparing the experimental results with the predictions of the semiempirical methods. It has been shown that the so far accepted assignment of the absorption band at 36 000 cm^{-1} of APO and DMAPO to the $S_2 \leftarrow S_0$ transition is wrong. We assign this absorption band to $S_1 \leftarrow S_0$ transition. Consequently, the photocycloreversion reaction of APO or DMAPO when excited with photons of energy ≥36 000 cm^{-1} occurs from the S_1 state, and hence such a photoreaction is not an exception to Kasha's rule. We have observed two new absorption bands at 47 000 and 56 000 cm^{-1}, which correlate excellently with the theoretical predictions. It has been shown that the spectroscopic signature of APO is closely related to the isoelectronic molecule 9,10-dihydro-9,10-ethanoanthracene (EA) and the electronic excited states of these molecules are governed by exciton-like interactions between the aromatic rings. We have shown that the HOMO and the LUMO of CPO are not of π^*_{OO} and σ^*_{OO} character, respectively, as assumed by Kearns and Khan.[5] It has been proposed that the dual photochemical behavior of APOs should be due to photochemistry occurring in the singlet and triplet manifolds, respectively. From the analysis of the semiempirical data of HCDPO, whose spectroscopic and photochemical behavior has been the basis for the so far accepted higher excited-state photocycloreversion of endoperoxides, we found that in HCDPO the carbonyl groups of anthrone subunits are responsible for the $S_1 \leftarrow S_0$ ($\pi^* \leftarrow n$) transition and the photocycloreversion may occur from a higher excited singlet state. Generalization of the observations on HCDPO to other endoperoxides which do not contain carbonyl groups, however, has been shown to be wrong.

There remain several questions to be clarified in the future. To mention a few, how the photocycloreversion occurs from the S_1 state of APO and DMAPO? Is there a barrier involved on this reaction pathway? If so, what is the magnitude of the barrier? Does the homolytic O−O bond cleavage of these endoperoxides occur from the triplet states and if so how? To answer these questions high-quality quantum chemical calculations are called for to map the potential energy hypersurface of the excited states of these molecules. Experimental investigations to exactly locate the 0−0 transition energy are warranted in order to estimate the magnitude of the barrier. Finally, thorough experimental and theoretical studies have to be carried out on

CPO itself. In light of the present work, assignments of the electronic states of other endoperoxides should be reexamined.

Acknowledgment. This work is financed by DFG in terms of the Habilitation Fellowship (GU 413/2-1 to 2-6) and a SPP (GU 413/3) to M.S.G. We thank Mr. Metzner and co-workers from the workshop of our institute for excellent workmanship. We also wish to thank Professor Axel Griesbeck for generously allowing us to use his laboratory facilities for the preparation of the endoperoxides. Travel funds from BESSY and excellent cooperation of Dr. W. Braun and Dr. G. Reichardt of BESSY are gratefully acknowledged.

References and Notes

(1) Adam, W.; Prein, M. *Acc. Chem. Res.* **1996**, *29*, 275.

(2) (a) Schmidt, R.; Drews, W.; Brauer, H.-D. *Z. Naturforsch.* **1982**, *37a*, 55. (b) Eisenthal, K. B.; Turro, N. J.; Dupuy, C. G.; Hrovat, D. A.; Langan, J.; Jenny, T. A.; Sitzmann, E. V. *J. Phys. Chem.* **1986**, *90*, 5168. (c) Drews, W.; Schmidt, R.; Brauer, H.-D. *Chem. Phys. Lett.* **1980**, *70*, 84.

(3) (a) Korolev, V. V.; Bolotsky, V. V.; Shokhirev, N. V.; Krissinel', E. B.; Bagryansky, V. A.; Bazhin, N. M. *Chem. Phys.* **1996**, *196*, 317. (b) Korolev, V. V.; Sushkov, D. G.; Bazhin, N. M. *Chem. Phys.* **1991**, *158*, 129.

(4) Kasha, M. *Discuss. Faraday Soc.* **1950**, *9*, 14.

(5) (a) Kearns, D. R.; Khan, A. U. *Photochem. Photobiol.* **1969**, *10*, 193. (b) Kearns, D. R. *J. Am. Chem. Soc.* **1969**, *91*, 6554.

(6) Rigaudy, J.; Breliere, C.; Scribe, P. *Tetrahedron Lett.* **1978**, *7*, 687.

(7) Schmidt, R.; Drews, W.; Brauer, H.-D. *J. Am. Chem. Soc.* **1980**, *102*, 2791.

(8) (a) Freyer, W.; Leupold, D. *J. Inf. Rec.* **1996**, *23*, 167. (b) Rigaudy, J. In *CRC Handbook of Organic Photochemistry and Photobiology*; Horspool, W. M., Song, P.-S., Eds.; CRC Press: Boca Raton, 1995; p 325.

(9) (a) Jesse, K.; Comes, F. J. *J. Phys. Chem.* **1991**, *95*, 1311. (b) Ernsting, N. P.; Schmidt, R.; Brauer, H.-D. *J. Phys. Chem.* **1990**, *94*, 5252. (c) Jesse, K.; Markert, R.; Comes, F. J.; Schmidt, R.; Brauer, H.-D. *Chem. Phys. Lett.* **1990**, *166*, 95. (d) Sitzmann, E. V.; Langen, J. G.; Hrovat, D. A.; Eisenthal, K. B. *Chem. Phys. Lett.* **1989**, *162*, 157. (e) Blumenstock, Th.; Jesse, K.; Comes, F. J.; Schmidt, R.; Brauer, H.-D. *Chem. Phys.* **1989**, *130*, 289. (f) Jesse, K.; Comes, F. J.; Schmidt, R.; Brauer, H.-D. *Chem. Phys. Lett.* **1989**, *160*, 8. (g) Blumenstock, Th.; Comes, F. J.; Schmidt, R.; Brauer, H.-D. *Chem. Phys. Lett.* **1986**, *127*, 452.

(10) Jesse, K. J. *Chem. Phys. Lett.* **1997**, *264*, 193.

(11) (a) Schaap, A. P.; Thayer, A. L.; Blossey, E. C.; Necker, D. C. *J. Am. Chem. Soc.* **1975**, *97*, 3741. (b) Wassermann, H. H.; Scheffer, J. R.; Cooper, J. L. *J. Am. Chem. Soc.* **1972**, *94*, 4991.

(12) Gudipati, M. S.; Kalb, M. *Chem. Phys. Lett.* **1997**, *268*, 169.

(13) Brown, C. J.; Ehrenberg, M. *Acta Crystallogr.* **1984**, *C40*, 1059.

(14) Frisch, M. J.; Trucks, G. W.; Schlegel, H. B.; Gill, P. M.; Johnson, B. G.; Robb, M. A.; Cheeseman, J. R.; Keith, T.; Petersson, G. A.; Montgomery, J. A.; Raghavachari, K.; Al-Laham, M. A.; Zakrzewski, V. G.; Ortiz, J. V.; Foresman, J. B.; Cioslowski, J.; Stefaov, B. B.; Nanayakkara, A.; Challacombe, M.; Peng, C. Y.; Ayala, P. Y.; Chen, W.; Wong, M. W.; Andres, J. L.; Replogle, E. S.; Comperts, R.; Martin, R. L.; Fox, D. J.; Binkley, J. S.; Defrees, D. J.; Baker, J.; Stewart, J. P.; Head- Gordon, M.; Gonzales, C.; Pople, J. A. *Gaussian 94*, revision D.3; *Gaussian, Inc.*: Pittsburgh, 1985.

(15) (a) Hartree, D. R. *Proc. Cambridge Philos. Soc.* **1928**, *24*, 89. (b) Fock, V. *Z. Phys.* **1930**, *61*, 126.

(16) (a) Del Bene, J.; Jaffé, H. H. *J. Chem. Phys.* **1968**, *48*, 1807, 4050; **1968**, *49*, 1221; **1969**, *50*, 1126. (b) Ellis, R. L.; Kuehnlenz, G.; Jaffé, H. H. *Theor. Chim. Acta* **1972**, *26*, 131.

(17) (a) Pople, J. A.; Beveridge, D. L.; Dobosh, P. A. *J. Chem. Phys.* **1967**, *47*, 2026. (b) Ridley, J.; Zerner, M. *Theor. Chim. Acta* **1973**, *32*, 111.

(18) Dick, B.; Hohlneicher, G. *Theor. Chim. Acta* **1979**, *53*, 221.

(19) Schmidt, R.; Schaffner. K.; Trost W.; Brauer, H.-D. *J. Phys. Chem.* **1984**, *88*, 956.

(20) (a) Gudipati, M. S.; Daverkausen, J.; Hohlneicher, G. *Chem. Phys.* **1993**, *173*, 143. (b) Gudipati, M. S.; Daverkausen, J.; Maus, M.; Hohlneicher, G. *Chem. Phys.* **1994**, *186*, 289. c) Gudipati, M. S.; Maus, M.; Daverkausen, J.; Hohlneicher, G. *Chem. Phys.* **1995**, *192*, 37.

(21) Gudipati, M. S. *J. Phys. Chem.* **1994**, *98*, 9750.

(22) Molina, V.; Merchán, M.; Roos, B. O. *J. Phys. Chem. A* **1997**, *101*, 3478.

(23) (a) Kolb, M.; Thiel, W. *J. Comput. Chem.* **1993**, *14*, 775. (b) Thiel, W. *Adv. Chem. Phys.* **1996**, *93*, 703.

(24) Turro, N. J. *Modern Molecular Photochemistry*; University Science Books: Sansaltio, 1991.

(25) (a) Kasha, M.; Rawls, H. R.; El-Bayoumi, M. A. *Pure Appl. Chem.* **1965**, *11*, 371. (b) Strickler, S. J.; Cormiev, R. A.; Connolly, J. S. *Int. J. Quantum Chem.* **1991**, *39*, 345. (c) Scholes, G. D.; Ghiggino, K. P.; Oliver, A. M.; Paddon-Row, M. N. *J. Am. Chem. Soc.* **1993**, *115*, 4345.

(26) Roos, B.; Andersson, K.; Fülscher, M. P. *Chem. Phys. Lett.* **1992**, *192*, 5.

(27) Li, Z.; Werner, A.; Schlögl, K. *Monatsh. Chem.* **1993**, *124*, 441.

(28) Cristol, S. J.; Aeling, E. O.; Strickler, S. J.; Ito, R. D. *J. Am. Chem. Soc.* **1987**, *109*, 7101.

(29) Klein, A.; Gudipati, M. S. Preliminary results.

(30) (a) Kobayashi, T.; Nagakura, S. *Chem. Phys. Lett.* **1976**, *43*, 429. (b) Garcia-Garibay, M. A.; Gamarnik, A.; Pang, L.; Jenks, W. S. *J. Am. Chem. Soc.* **1994**, *116*, 12095. (c) Shimada, R.; Goodman, L. *J. Chem. Phys.* **1965**, *43*, 2027.